

STRUCTURAL CONSEQUENCES OF GROUT DETERIORATION IN THE GROUTED SHEAR STUD (GSS) CONNECTION

Arjun, Jayaprakash^{1*}, James, Nau², Mohammad, Pour-Ghaz³ and Mervyn, Kowalsky⁴

¹: PhD Candidate, NC State University, Raleigh, USA; email: ajayapr@ncsu.edu

²: Professor, NC State University, Raleigh, USA; email: nau@ncsu.edu

³: Associate Professor, NC State University, Raleigh, USA; email: mpourgh@ncsu.edu

⁴: Professor, NC State University, Raleigh, USA; email: kowalsky@ncsu.edu

*: corresponding author

Keywords: Grouted Shear Stud connection; Large scale testing; Artificial damage simulation; Steel bridge substructures; Seismic design

Abstract: The grouted shear stud (GSS) connection for steel bridge substructures was developed, for utility in seismic design, as a ductile alternative to the column to cap-beam directly welded connection. The GSS connection utilizes plastic hinge relocation to eliminate brittle cracking at the weld region and provides full strength and ductility capacity for steel bridge columns. However, the grout material used as part of the GSS connection is susceptible to damage through years of exposure, especially in extremely cold climates. This study investigates the effect of grout deterioration on the overall structural behavior of steel bridge substructure systems by artificially simulating grout damage states in a series of large-scale tests. This paper discusses preliminary results from two large scale tests performed on two-column steel bridge bent specimens. The first was a control specimen which was a newly constructed bridge bent that utilized the GSS connection. Expanded polystyrene beads were added to the grout in the GSS connection for the second specimen to simulate a state of damage caused by cold-climate exposure, i.e., a reduced strength and stiffness. Preliminary results indicate that the global behavior of steel bridge substructures are not significantly affected by grout deterioration in the GSS connection.

1. Introduction

The Grouted Shear Stud (GSS) connection is a steel bridge column-to-cap beam connection with potential use in seismic design. The components of the GSS connection include a round steel pile column, a steel pipe stub of larger diameter, and a steel cap beam as shown in Fig. 1(a). The pipe stub is shop welded to the cap beam. The cap beam-stub assembly is then lowered onto the erected piles to make a socket type connection. The annular region between the pile and larger diameter pipe stub is then filled with high strength grout to complete the connection. In contrast to conventional column-to-cap beam directly welded connections, the GSS connection relocates the plastic hinge to the steel column section thereby mobilizing its full capacity and ductility before failure. Complete discussion of the GSS connection may be found in Fulmer et al. (2015, 2016). This paper summarizes two large scale tests of two-column steel bent specimens that incorporate the GSS connection. The objective of these tests was to determine if damage to the GSS connection due to long-term exposure to extreme cold climatic conditions could potentially reduce the seismic

performance of the bent. Each test utilizes a different level of deterioration (LoD) for the grout in its connections, i.e., damage states are simulated for the GSS connection in each test. Differences in their performance under cyclic quasi-static lateral loading were investigated. The first test was a control test. The GSS connections in the first test specimen were initially undamaged. The second test had GSS connections that had reduced grout compressive strength (f'_c) and elastic modulus (E) representative of a moderate-to-high level damage due to freeze-thaw exposure.

2. Experimental Setup

The test specimens were large scale two-column steel bents as shown in Fig. 1(b). The steel bent was supported by two base shoes through pin connections. The height of the center of the cap-beam from the pins was 11 ft 2 in (3.40 m) and the center-to-center distance between the two columns was 12 ft (3.66 m). The base shoes were prestressed to the laboratory strong floor using 1-3/8 in (35 mm) diameter Dywidag bars. A 440-kip (1957 kN) actuator mounted on the laboratory strong wall was used to apply quasi-static cyclic lateral loading. A three-cycle-set loading history was chosen. To make meaningful comparisons, both tests followed the same displacement history. After initial elastic cycles, three cycles at each ductility level (μ_1 , $\mu_{1.5}$, μ_2 , μ_3 and so on) were applied until test termination. The criterion for termination was either rupture of the pile column wall or an overall strength drop below 50%.



(a)

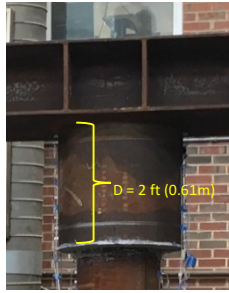


(b)

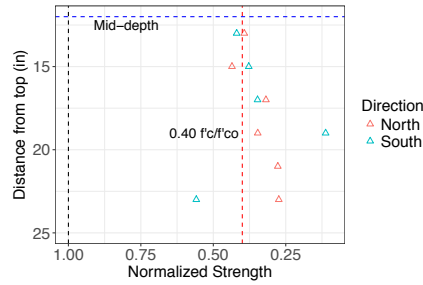
Fig. 1. (a) Constituents of the GSS connection; (b) Experimental setup for Tests 1 and 2.

3. Artificial Damage Simulation for Test 2

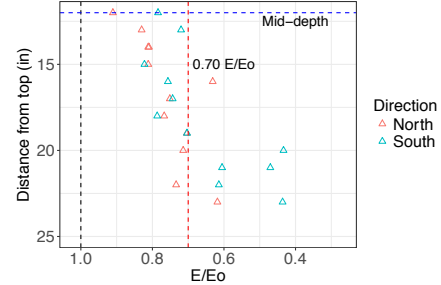
Years of exposure in a cold climate tend to reduce the structural properties, such as compressive strength (f'_c) and elastic modulus (E), of cementitious grouts. Simulating this reduction in grout properties to effectively represent the long-term damage state of grout was essential to define the level of deterioration (LoD) variable for Test 2. A few studies (Babu et al. 2005, Bucher 2009) in the past have found that adding expanded polystyrene (EPS) beads to a cementitious mixture could reduce its structural properties E and f'_c . Therefore, the addition of EPS was the chosen method to simulate reduced properties for this study. Note that LoD in these tests refers to the state of the bottom half of the GSS connections with respect to parameters f'_c and E. Almost all of the durability damage is assumed to be focused in the bottom half of the connection. Moreover, the contribution of the top half of the connection in force transfer is likely low. Fig. 2 shows the state of the grout in the connections of the Test 2 specimen. The y-axis is the depth of the location of measurement from the bottom of the cap beam. The x-axis show values of compressive strength in Fig. 2(b) and elastic modulus in Fig. 2(c) normalized to the same quantities in Test 1. Compressive strength of 2 in x 2 in (50 mm x 50 mm) cubic samples taken during casting was measured per ASTM C109 (2018). The elastic modulus was measured from disc samples using



(a)



(b)



(c)

Fig. 2. Results of grout properties from the GSS connection of Test 2: (a) GSS connection depth; (b) Compressive strength profile obtained from cubic samples; (c) Dynamic elastic modulus profile obtained from disc samples; (1 in = 25.4 mm).

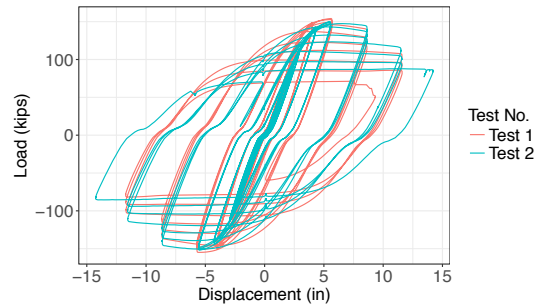
the method proposed by Leming et al. (1998). On average, the GSS connections in Test 2 had a reduction in strength of 60% and elastic modulus of 30% compared to Test 1 in the bottom half of the connection.

4. Results and Discussion

Test 1 achieved a drift of 9% while Test 2 achieved 11% drift as shown in Fig. 3(a). A comparison of the cyclic force-displacement hysteresis curves for the two tests is shown in Fig. 3(b). Tests 1 and 2 showed similar structural behavior. During the elastic cycles, Test 2 specimen had a slightly reduced stiffness compared to Test 1 specimen as shown in Fig. 4(a). This was expected since the grout in Test 2 had a lower elastic modulus. However, this reduction is only slightly noticeable in the complete force-displacement hysteresis curve. In the early inelastic cycles ($\mu 1$ and $\mu 2$), the curvature demand in the plastic hinge region for Test 1 columns was higher than that of Test 2. This resulted in a slightly larger energy dissipation by Test 1 specimen compared to Test 2 as shown in Fig. 4(b). During $\mu 3$ cycles, shown in Fig. 4(c), Test 1 specimen started losing its load carrying capacity as the plastic hinge was fully developed. The section just below the plastic hinge pinched and therefore reduced the section modulus. Moreover, high strain demands caused the steel material to yield and thereby reduced the wall thickness. During $\mu 4$ cycles, shown in Fig. 4(d), both Test 1 and Test 2 started to show similar behavior once again. Some differences here included a slightly higher load carrying capacity and a reduced reloading stiffness of Test 2 specimen. Loosely speaking, Test 2 specimen was more flexible and ductile than Test 1 specimen.



(a)



(b)

Fig 3. (a) The maximum drift achieved by Test 2 was 11% at a ductility of 5; (b) A comparison of the force-displacement hysteresis of two tests; (1 in = 25.4 mm, 1 kip = 4.45 kN).

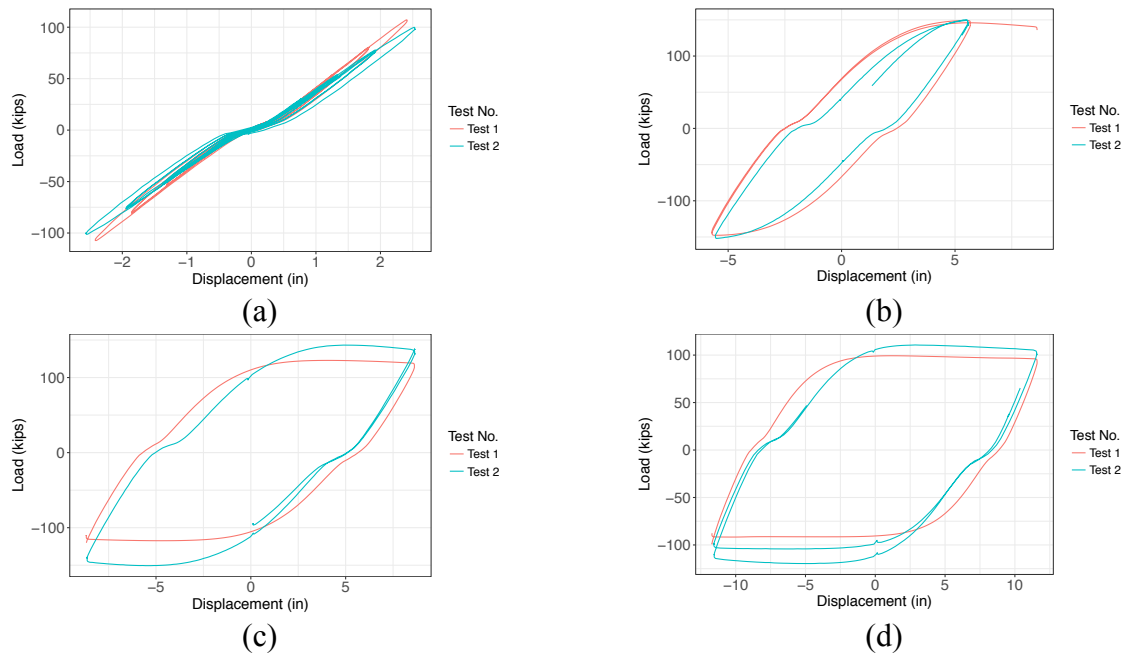


Fig. 4. Comparison for hysteretic loops at different ductilities: (a) F_y cycles; (b) μ_2 cycles; (c) μ_3 cycles; (d) μ_4 cycles; (1 in = 25.4 mm, 1 kip = 4.45 kN).

Despite the grout properties being reduced considerably, the difference in the overall structural behavior of the two-column bent specimens was of no practical significance. Results suggest that a moderate-to-high level of durability damage within the GSS connection in steel bridge substructures is of little concern from the perspective of its global structural behavior under lateral loading. However, this cannot be stated conclusively without further investigation. Two additional large scale tests of similar nature are planned to be executed in March-April 2019.

5. References

- ASTM C109. 2016. Standard Test Method for Compressive Strength of Hydraulic Cement Mortar, ASTM International, West Conshohocken, PA.
- Babu, D.S., Babu, K.G., and Wee, T. 2005. Properties of lightweight expanded polystyrene aggregate concretes containing fly ash. *Cement and Concrete Research* **35**(6), 1218-1223.
- Bucher, B.E. 2009. Shrinkage and shrinkage cracking behavior of cement systems containing ground limestone, fly ash, and lightweight synthetic particles. Thesis, Purdue University.
- Fulmer, S., Kowalsky, M., and Nau, J. 2015. Grouted shear stud connection for steel bridge substructures. *Journal of Constructional Steel Research* **109**, 72-86.
- Fulmer, S.J., Nau, J.M., Kowalsky, M.J., and Marx, E. 2016. Development of a ductile steel bridge substructure system. *Journal of Constructional Steel Research* **118**, 194-206.
- Leming, M.L., Nau, J.M., and Fukuda, J. 1998. Non-destructive determination of dynamic modulus of concrete disks. *Materials Journal* **95**(1), 50-57.